Mercury-Free Preparation, Characterization, and Molecular Structure of Tricyanovinylferrocene Using an Unusual Reaction between Ferrocene and Tetracyanoethylene

Victor N. Nemykin,* Alexander Y. Maximov, and Alexey Y. Koposov

Department of Chemistry & Biochemistry, University of Minnesota Duluth, Duluth, Minnesota 55812

Received February 21, 2007

A direct reaction between ferrocene (FcH) and tetracyanoethylene (TCNE) in various solvents and within a wide range of temperatures has been investigated in order to optimize the preparation of tricyanovinylferrocene. Under optimized reaction conditions, tricyanovinylferrocene was prepared in ~26% yield along with cyanoferrocene as a major reaction product in the reaction between 1 equiv of FcH and 2 equiv of TCNE for 10 min in sulfolane at 110 °C. It was proposed that the reaction proceeds via a single-electron-transfer step, which results in the formation of a spectroscopically detected $[FcH]^{\bullet+}[TCNE]^{\bullet-}$ intermediate followed by homolytic cleavage of the C−CN bond. The possible phase transition in tricyanovinylferrocene has been tested by X-ray crystallography at 173 and 293 K. The prominent visible band observed in the UV−vis spectrum of tricyanovinylferrocene has been unambiguously assigned to a metal-to-ligand charge-transfer transition on the basis of experimental and theoretical (TDDFT) data, while its solvatochromic behavior was tested using the Kamlet−Taft model. It has been found that the solvatochromism observed in tricyanovinylferrocene predominantly depends on the value of dipolarity/polarizability parameter π^* in the Kamlet−Taft equation. The significant anisotropy of the quadrupole doublet in the Mössbauer spectra of tricyanovinylferrocene and cyanoferrocene was explained on the basis of DFT calculations.

Introduction

Ferrocene-containing porphyrins and phthalocyanines have been intensively investigated during the last few decades primarily because of their potential applications in switchable molecular optical and electronic nanodevices.[1] Recently, we have shown that the magnesium complex of 2(3),7(8),12(13),-17(18)-tetracyano-3(2),8(7),13(12),18(17)-tetraferrocenyl-5,10,-15,20-tetraazaporphyrin has unusual optical properties in the near-IR region, which can be useful for practical applications in optical limiting devices.[2] This tetraazaporphyrin was prepared by template tetramerization of the so far poorly characterized tricyanovinylferrocene (**1**), the common synthesis of which requires the use of a highly toxic chloromercurioferrocene precursor.[2,3] In order to avoid the use of costly or highly toxic reagents for the preparation of **1**, we examined in detail the direct tricyanovinylation reaction between ferrocene and tetracyanoethylene in variety of solvents and under different reaction conditions and have found a simple way for the preparation of **1** in large quantities and high purity. In addition, spectroscopic properties, molecular structure, and solvatochromism of complex **1** were carefully investigated by various experimental and theoretical approaches.

Experimental Section

Preparation of Compounds. The synthesis of ferrocenyl-containing complexes was carried out in an oxygen-free dry argon atmosphere using dry degassed solvents. Ferrocene and tetracyanoethylene were purchased from TCI and used without further purification. Solvents were purchased either from Aldrich Chemical Co. or Acros Chemical Co. and purified by distillation as follows: acetonitrile from CaH_2, followed by Li_2CO_3−$KMnO_4$, and finally from P_2O_5; CH_2Cl_2, $CHCl_3$, and butyronitrile from CaH_2; toluene from sodium-benzophenone; ethanol from sodium ethoxide; sulfolane, DMF, and DMSO by distillation over molecular sieves (4 Å) under reduced pressure. Silica gel (60 Å, 70−230 mesh) was purchased from Sorbent Technologies.

Synthesis of Tricyanovinylferrocene (1) and Cyanoferrocene (2). Method A. A 1.28 g (10 mmol) portion of tetracyanoethylene was added to a preheated (100 °C) solution of 0.93 g (5 mmol) of ferrocene in 10 mL of sulfolane. Immediately after addition, the color of the solution changed first to green and later to blue. The reaction mixture was heated continually with stirring for 10 min, and then, it was cooled to room temperature. The resulting solution was poured into 50 mL of water, and the obtained precipitate was filtered and washed several times with water. The resulting dark brown-black powder was dissolved in CH_2Cl_2, filtered, and purified by column chromatography on silica gel using 4:1 toluene/hexane as an eluent. The first, yellow band contains unreacted ferrocene as confirmed by ^1H and ^{13}C NMR spectra. The second, orange band consists of pure cyanoferrocene **2**, while the third, dark blue band is the target compound **1**. All three products were collected and the solvent was evaporated, yielding ferrocene (102 mg, 11%), cyanoferrocene **2** (390 mg, 37%), and tricyanovinylferrocene **1** (120 mg, 8.4%), respectively. Complex **1**: mp 130−131 °C (hexane,

* Author to whom correspondence should be addressed. E-mail: vnemykin@d.umn.edu.

(1) Schmidt, E. S.; Calderwood, T. S.; Bruice, T. C. *Inorg. Chem.* **1986**, *25*, 3718. Uosaki, K.; Kondo, T.; Zhang, X. Q.; Yanagida, M. *J. Am. Chem. Soc.* **1997**, *119*, 8367. Boyed, P. D.; Burrell, A. K.; Campbell, W. M.; Cocks, P. A.; Gordon, K. C.; Jameson, G. B.; Officer, D. L.; Zhao, Z. *Chem. Commun.* **1999**, 637. Baumann, T. F.; Nasir, M. S.; Sibert, J. W.; White, A. J. P.; Olmstead, M. M.; Williams, D. J.; Barrett, A. G. M.; Hoffman, B. M. *J. Am. Chem. Soc.* **1996**, *118*, 10479. Jin, Z.; Nolan, K.; McArthur, C. R.; Lever, A. B. P.; Leznoff, C. C. *J. Organomet. Chem.* **1994**, *468*, 205. Poon, K.-W.; Yan, Y.; Li, X.; Ng, D. K. P. *Organometallics* **1999**, *18*, 3528.

(2) Nemykin, V. N.; Kobayashi, N. *Chem. Commun.* **2001**, 165.

(3) Perevalova, E. G.; Lemenovskii, D. A.; Alekseev, V. P.; Grandberg, K. I.; Nesmeyanov, A. N. *Izv. Acad. Nauk SSSR, Ser. Khim.* **1972**, *8*, 1867.

10.1021/om070160k CCC: $37.00
Publication on Web 05/19/2007

Table 1. Optimization of Experimental Conditions for Preparation of Complex 1

entry	solvent	*T* (°C)	*t* (min)	FcH (mmol)	TCNE (mmol)	purification method[a]	yield of **1** (%)
1	sulfolane	150	10	5	5	A	<1[b]
2	sulfolane	130	10	5	5	A	<1[b]
3	sulfolane	120	10	5	5	A	4.2
4	sulfolane	120	10	5	7.5	A	4.9
5	sulfolane	120	10	5	10	A	7.8
6	sulfolane	110	10	5	10	A	8
7	sulfolane	100	10	5	10	A	8.4
8	sulfolane	100	5	10	20	B	18
9	sulfolane	100	10	10	20	B	25.8
10	DMF	110	10	5	10	B	<1[b]
11	DMSO	110	10	5	10	B	<1[b]
12	acetonitrile	reflux	180	5	10	C	2.2
13	butyronitrile	reflux	30	5	10	C	2.3

[a] Purification methods are described in the Experimental Section. [b]Trace amounts of the product were detected by UV−vis spectroscopy after purification.

Table 2. Crystallographic Data of Compounds 1 and 2

	compound **1** 293 K	compound **1** 173 K	compound **2**
formula	$C_{15}H_9N_3Fe_1$	$C_{15}H_9N_3Fe_1$	$C_{11}H_9N_1Fe_1$
cryst class	monoclinic	monoclinic	orthorhombic
space group	$P2_1/m$	$P2_1/m$	$P2_12_12_1$
cell params			
a, Å	6.989(2)	6.9460(14)	7.6320(15)
b, Å	9.907(3)	9.800(2)	10.454(2)
c, Å	9.688(2)	9.6527(19)	11.228(2)
β, deg	106.35(2)	106.26(3)	90.0
volume, Å^3	643.7(3)	630.8(2)	895.8(3)
Z	2	2	4
radiation type	Mo Kα	Mo Kα	Mo Kα
cryst size, mm	0.17 × 0.33 × 0.48	0.10 × 0.15 × 0.22	0.28 × 0.41 × 0.49
no. of reflns measd	1981	2553	1659
no. of indep reflns	1974	1371	1641
no. of reflns used	1805 ($\sigma \geq 3$)	926 ($\sigma \geq 3$)	1511 ($\sigma \geq 3$)
2θ range	4−60	4−55	5−60
R_f	0.0324	0.0332	0.0254
R_w	0.0597	0.0625	0.0607
no. of params	135	122	146
goodness of fit	1.1690	0.9384	0.9419

lit. 125−127 °C,[4] 134−135 °C[5]). ^{1}H NMR (500 MHz, $CDCl_3$): δ 5.27 (t J = 1.5 Hz, 2H, α-Cp_1); 5.165 (t J = 1.5 Hz, 2H, β-Cp_1); 4.47 (s, 5H, Cp_2). ^{13}C NMR (125 MHz, $CDCl_3$): δ 143.98 (C═C), 113.74 (CN), 113.63 (CN), 113.22 (CN), 79.78 (C═C), 77.79 (α-C, Cp_1), 75.24 (*i*-C, Cp_1), 73.19 (Cp_2), 72.15 (β-C, Cp_1). IR (cm^{-1}, KBr): 3100 w (Cp-H), 2222 s (CN), 1526 vs (C═C), 1450 s, 1411 s, 1381 m, 1350 m, 1334 m, 1294 s, 1224 m, 1076 m, 1044 m, 1022 m, 998 s, 931 m, 860 m, 825 s, 816 s, 693 s; UV−vis (λ_{max}, nm (log ϵ), $CHCl_3$): 363 (4.04), 628 (3.43). Anal. Calcd for $C_{15}H_9N_3Fe$: C, 62.75, H, 3.16, N, 14.64. Found: C, 63.13, H, 3.31, N, 14.14. Compound **2**: mp 106 − 108 °C (lit 108[5]). ^{1}H NMR (500 MHz, $CDCl_3$): δ 4.65 (t J = 1.5 Hz, 2H, α-Cp_1); 4.39 (t J = 1.5 Hz, 2H, β-Cp_1); 4.34 (s, 5H, Cp_2). ^{13}C NMR (125 MHz, $CDCl_3$): δ 120.20 (CN), 77.68 (α-C, Cp_1), 70.69 (β-C, Cp_1), 70.54 (Cp_2), 51.78 (*i*-C, Cp_1). ^{13}C NMR (125 MHz, DMSO-d_6): δ 120.12 (CN), 71.57 (α-C, Cp_1), 70.95 (β-C, Cp_1), 70.28 (Cp_2), 51.05 (*i*-C, Cp_1). IR (cm^{-1}, KBr): 3092 s (Cp-H), 2224 s (CN), 1410 s, 1230 s, 1106 m, 1028 s, 1003 s, 911 m, 844 s, 817 s, 552 s. Anal. Calcd for $C_{11}H_9NFe$: C, 62.60, H, 4.30, N, 6.64. Found: C, 62.71, H, 4.27, N, 6.66.

Method B. A 2.56 g (20 mmol) sample of tetracyanoethylene was added to a preheated (100 °C) solution of 1.86 g (10 mmol) of ferrocene in 20 mL of sulfolane. Immediately after addition, the color of the solution changed first to green and later to blue. The reaction mixture was heated continually with stirring for 10 min, and then, it was cooled to room temperature. The resulting solution was poured into 50 mL of water, and the reaction products were immediately extracted using toluene/hexane (1:1 v/v) as a solvent. The organic layer was washed several times with water, dried over $CaCl_2$, and evaporated to dryness. The target compound **1** was purified as described for method A. Yield: 740 mg (25.8%).

Method C. A 1.28 g (10 mmol) amount of tetracyanoethylene was added to a solution of 0.93 g (5 mmol) of ferrocene in 20 mL of appropriate solvent. A green reaction mixture was refluxed or heated at 110 °C for the time indicated in Table 1, following by evaporation of the solvent at reduced pressure. Compound **1** (with the yield shown in Table 1) was obtained using column chromatography as described in method A above.

Spectroscopic Measurements. UV−vis spectra were recorded on a temperature-controlled Hewlett-Packard 8453 spectrophotometer. NMR data were collected using a Varian INOVA-500 spectrometer with 500 MHz frequency for protons and 125 MHz frequency for carbon experiments. Chemical shifts are reported in parts per million and referenced to TMS as an internal standard. IR spectra were recorded on a Perkin-Elmer FT-IR 1760X spectrometer in KBr pellets. Elemental analysis was done at Atlantic Microlab Inc. (Atlanta). Electrochemical measurements were conducted using a CH electrochemical analyzer utilizing a three-electrode scheme with platinum working and auxiliary electrodes and a Ag/AgCl reference pseudoelectrode in 0.1 M solution of

(4) Freeman, M. B.; Sneddon, L. G. *Inorg. Chem.* **1980**, *19*, 1125.
(5) Nefedov, V. A.; Bespalov, B. P.; Titov, V. V. *Zh. Org. Khim.* **1974**, *10*, 1553.

Scheme 1. Synthetic Procedures for the Preparation of Complex 1[a]

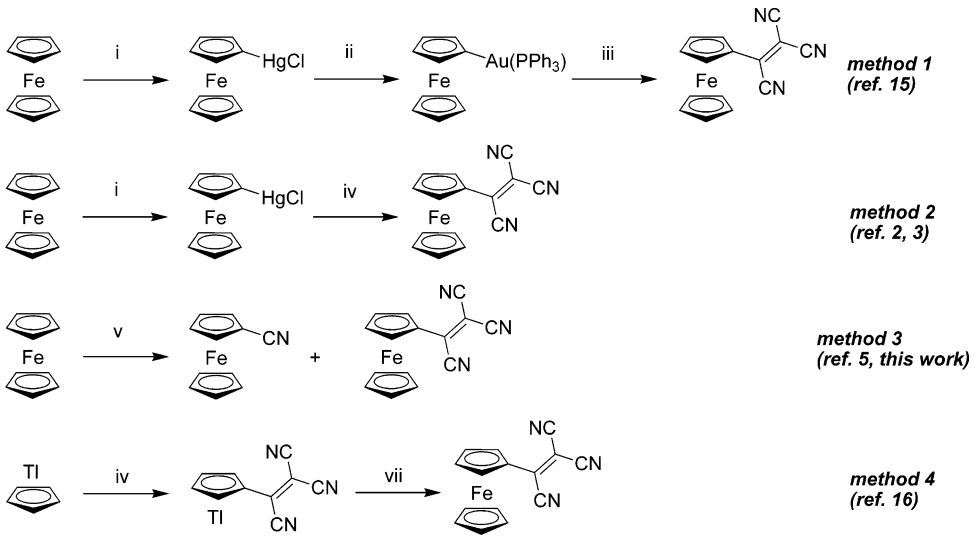

[a] (i) $Hg(OAc)_2$/KCl; (ii) $AuCl(PPh_3)$; (iii) TCNE, C_6H_6, reflux; (iv) TCNE, acetonitrile, reflux; (v) TCNE, sulfolane, 150 °C; (vi) TCNE, acetonitrile, 0 °C; (vii) $Fe(CO)_2I$.

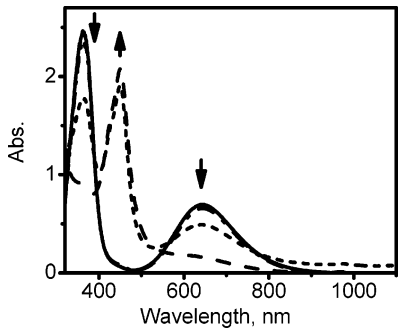

Figure 1. Degradation of complex **1** in a sulfolane/water (98:2 v/v) mixture within 48 h.

TBAP in acetonitrile with redox potentials corrected using an internal standard (ferrocene) in all cases.

X-ray Structure Determination. Crystals of tricyanovinylferrocene **1** (CCDC reference number 643479, 293 K; 643480, 173 K) were obtained by slow diffusion of hexane into saturated CH_2Cl_2 or $CHCl_3$ solutions of the crude compound at room temperature following by slow evaporation of the resulting mixture. This approach provided well-shaped dark blue colored X-ray quality single crystals. Intensity data were collected using a Rigaku AFC-7R diffractometer at room temperature and Bruker APEX CCD diffractometer at −100 °C with Mo Kα radiation and a graphite monochromator in both cases. A total of 1981 or 2553 reflections were collected ($\theta = 2.5-30.0°$); of these 1974 and 1371 reflections were unique for room- and low-temperature experiments, respectively. The data were corrected for absorption using the ψ-scan (room-temperature experiment) or DIFABS (low-temperature experiment) method. All raw data were processed using the TeXsan 10.3b[6] (room-temperature experiment) or ShelXTL (low-temperature experiment) program. The structures were solved by the Patterson method and refined by full-matrix least-squares procedures on F^2 using the Crystals for Windows program.[7] The three-parameter Prince-modified Chebychev polynomial weighting scheme incorporated in the program was used for the refinement. All nonhydrogen atoms were refined anisotropically, while the hydrogen atoms were found in calculated positions and refined using the riding model. Crystals of cyanoferrocene **2** (CCDC reference number 643481) were obtained by slow evaporation of a saturated $CHCl_3$ solution at room temperature. Intensity data were collected using a Rigaku AFC-7R diffractometer at room temperature with Mo Kα radiation and a graphite monochromator. A total of 1659 reflections were collected ($\theta = 2.5-30.0°$); of these, 1641 reflections were unique. The data were corrected for absorption using the ψ-scan method. All raw data were processed using the TeXsan 10.3b[6] program. The structures were solved by the Patterson method and refined by full-matrix least-squares procedures on F^2 using the Crystals for Windows program.[7] The three-parameter Prince-modified Chebychev polynomial weighting scheme incorporated in the program was used for the refinement. All nonhydrogen atoms were refined anisotropically, while the hydrogen atoms were found in calculated positions and refined using the riding model. The important crystallographic data on complexes **1** and **2** are presented in Table 2.

Computational Details. All computations were performed using the Gaussian 03[8] software package running under Windows or UNIX OS. X-ray geometries were used for compounds **1** and **2** as well as the D_{5h} geometry for ferrocene. The excitation energies were calculated by the TDDFT approach with the lowest 40 singlet excited states being considered. The ^{57}Fe quadrupole splittings and isomer shifts in **1** and **2** were calculated as described previously.[9] In all calculations, Becke's exchange functional[10] and the Pedrew−Wang correlation functional[11] (BPW91) were used. Wachter's full-electron basis set was used for iron,[12] while for all other atoms the 6-311G(d)[13] basis set was employed. This combination of exchange−correlation functional and basis set was found to be dramatically better in the calculation of spectroscopic parameters in ferrocene-containing systems as compared to the more popular hybrid exchange−correlation functionals, i.e., B3LYP.[9] The percentage of

(6) *TeXsan* 10.3.b; Rigaku Inc., 1998.
(7) Betteridge, P. W.; Carruthers, J. R.; Cooper, R. I.; Prout, K.; Watkin, D. J. *J. Appl. Crystallogr.* **2003**, *36*, 1487.
(8) Frisch, M. J.; Trucks, G. W.; Schlegel, H. B.; Gill, P. M. W.; Johnson, B. G.; Robb, M. A.; Cheeseman, J. R.; Keith, T. A.; Petersson, G. A.; Montgomery, J. A.; Raghavachari, K.; Al-Laham, M. A.; Zakrzewski, V. G.; Ortiz, J. V.; Foresman, J. B.; Cioslowski, J.; Stefanov, B. B.; Nanayakkara, A.; Challacombe, M.; Peng, C. Y.; Ayala, P. Y.; Chen, W.; Wong, M. W.; Andres, J. L.; Replogle, E. S.; Gomperts, R.; Martin, R. L.; Fox, D. J.; Binkley, J. S.; Defrees, D. J.; Baker, J.; Stewart, J. P.; Head-Gordon, M.; Gonzalez, C.; Pople, J. A. *Gaussian 03*; Gaussian, Inc.: Pittsburgh, PA, 2003.
(9) Nemykin, V. N.; Hadt, R. G. *Inorg. Chem.* **2006**, *45*, 8297.
(10) Becke, A. D. *Phys. Rev. A* **1988**, *38*, 3098.
(11) Perdew, J. P.; Wang, Y. *Phys. Rev. B* **1992**, *45*, 13244.
(12) Wachters, A. J. H. *J. Chem. Phys.* **1970**, *52*, 1033.

Scheme 2. Proposed Mechanism for Tricyanovinylation of TlCp[4]

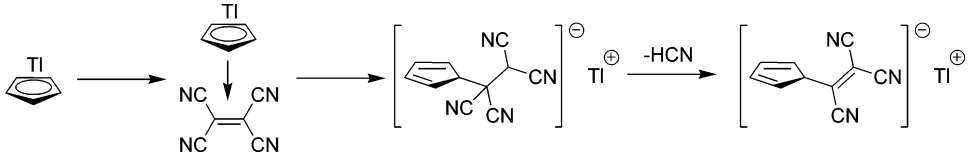

Scheme 3. Possible External Radical-Initiated Mechanism of TCNE Dissociation

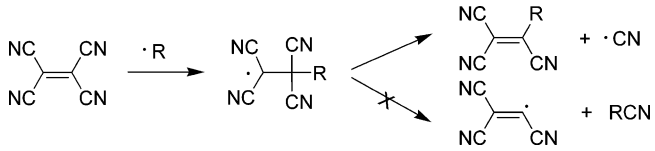

Scheme 4. Possible Single-Electron-Transfer Mechanism for the Formation of Complexes 1 and 2 in the Reaction between FcH and TCNE

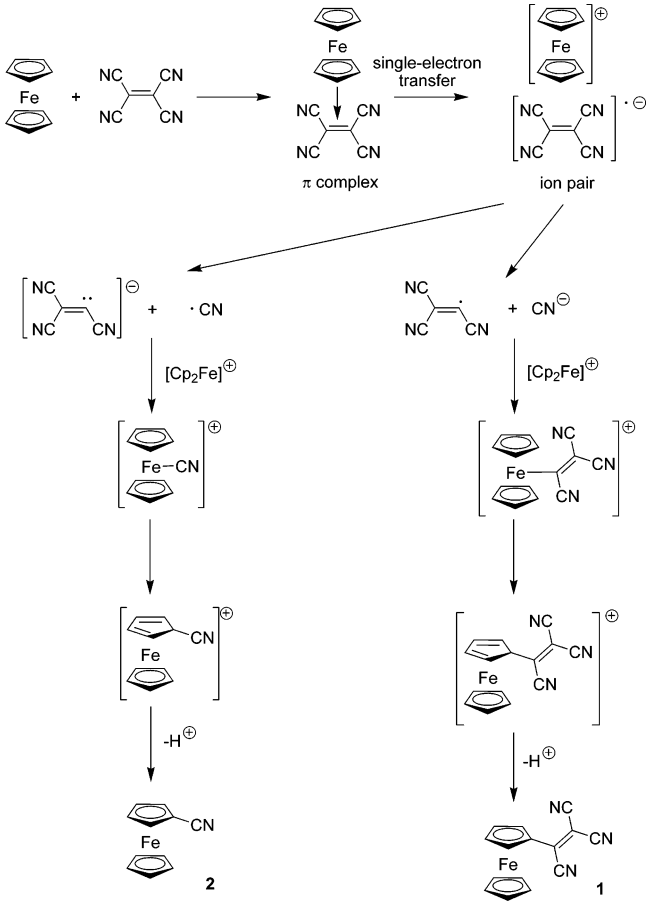

atomic orbital contributions to their respective molecular orbitals was calculated by using the VMOdes program.[14]

Results and Discussion

1. Optimization of Reaction Conditions for the Preparation of 1 in the Reaction between Ferrocene and Tetracyanoethylene. The known synthetic procedures for the preparation of **1** are summarized in Scheme 1. Thus, the highest overall yield of 58% in the preparation of complex **1** can be achieved in a three-step approach that involves environmentally dangerous chloromercuration of ferrocene followed by transformation of chloromercurioferrocene into expensive triphenylphosphinatoaurioferrocene, which can be tricyanovinylated by TCNE in high yield (method 1, Scheme 1).[15] It is possible to eliminate one step in the above-mentioned synthetic route by using direct tricyanovinylation of chloromercurioferrocene by TCNE with the overall yield of target compound **1** of 32% (method 2, Scheme 1).[2,3] Alternative preparation of **1** requires tricyanovinylation of highly toxic thallium cyclopentadienide followed by interaction of thallium tricyanovinylcyclopentadiene with cyclopentadienyliron dicarbonyl iodide with an overall yield of only 3.6% (method 4, Scheme 1).[4,16] Finally, in a very brief half-page note it was mentioned that the direct 10 min reaction between ferrocene and TCNE in sulfolane at 150 °C can produce tricyanovinylferrocene in 16% yield (method 3, Scheme 1).[5]

Such a direct tricyanovinylation of ferrocene can be a good alternative for the preparation of tricyanovinylferrocene because this one-step reaction utilizes inexpensive reagents and does not involve toxic mercury- or thallium-containing precursors. In our hands, however, the 10 min reaction between equimolar amounts of FcH and TCNE conducted at 150 °C produced black uncharacterized tar as the major product with only a trace amount of target tricyanovinylferrocene **1**. Reduction of the reaction temperature to 130 °C did not improve the situation. However, the desired compound **1** was separated in low (4.2%) yield when the same reaction was conducted at 120 °C. Encouraged by this result, we tried to change the reactant ratio by increasing the relative amount of TCNE introduced into the reaction. Indeed, the yield of the tricyanovinylferrocene increased to 4.9% and 7.8% when a 1:1.5 and 1:2 FcH:TCNE ratio was used, respectively (Table 1). A further decrease in temperature to 100 °C, keeping a 1:2 ratio of reagents, produces the target complex in 8.4% yield. During purification of the target complex, we found that precipitation of the reaction products from sulfolane solution into water led to the formation of a large amount of red-colored uncharacterized material initially absent in the reaction mixture. This material has a UV−vis spectrum similar to that obtained when the pure **1** in sulfolane/water (98:2 v/v) solution undergoes prolonged exposure to air (Figure 1).

Taking into consideration the possibility of degradation of the tricyanovinylferrocene in the presence of air in a polar organic solvent−water media, we tried to change the purification procedure in the tricyanovinylation reaction of ferrocene in two

(13) McLean, A. D.; Chandler, G. S. *J. Chem. Phys.* **1980**, *72*, 5639. Krishnan, R.; Binkley, J. S.; Seeger, R.; Pople, J. A. *J. Chem. Phys.* **1980**, *72*, 650.

(14) Nemykin, V. N.; Basu, P. *VMOdes*: Virtual Molecular Orbital description program for Gaussian, GAMESS, and HyperChem, Revision A 7.1; 2003.

(15) Perevalova, E. G.; Lemenovskii, D. A.; Alekseev, V. P.; Grandberg, K. I.; Nesmeyanov, A. N. *Izv. Acad. Nauk SSSR, Ser. Khim.* **1972**, *8*, 1869.

(16) Freeman, M. B.; Sneddon, L. G.; Huffman, J. C. *J. Am. Chem. Soc.* **1977**, *99*, 5194.

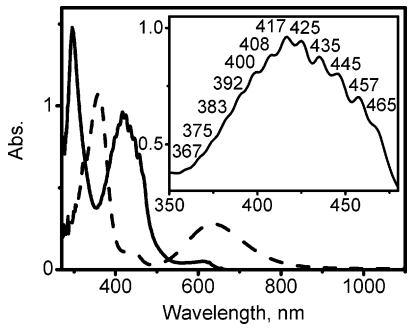

Figure 2. UV−vis spectra of complex **1** (dashed line) and FcH treated with TCNE in acetonitrile at 80 °C (solid line).

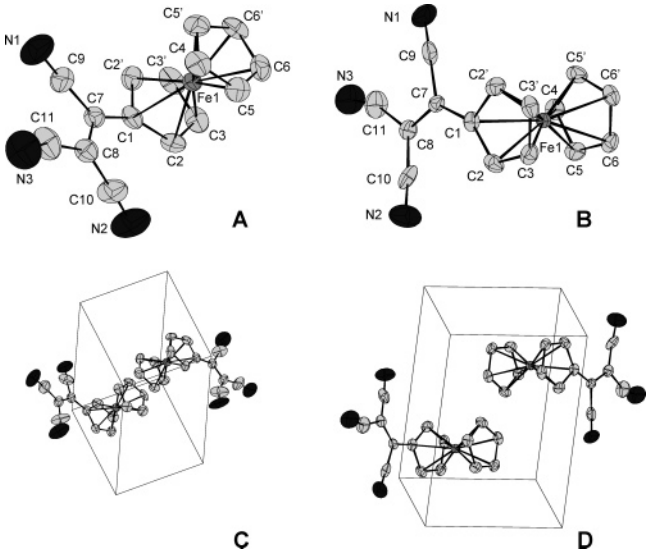

Figure 3. Molecular structure of complex **1** at 293 K (A, C) and 173 K (B, D).

ways. First, we tried to directly load the reaction mixture on the chromatographic column and elute sulfolane with hexane first, but this approach turned out to be highly unreliable and did not allow us to prepare the target compound in the pure state. In the second modification (mentioned as method B in Table 1) the reaction solution was first diluted with toluene/hexane (1:1 v/v) mixture, and then, sulfolane was extracted with water. This modification affords compound **1** in 25.8% yield, which is close to the total yield of the two-step approach involving highly toxic chloromercurioferrocene (method 2, Scheme 1).[2,3] Since the choice of sulfolane as the solvent for the direct tricyanovinylation reaction of ferrocene was not obvious, we also tested several other solvents (Table 1). In the case of common dipolar aprotic solvents, i.e., DMSO and DMF, only a trace amount of compound **1** was obtained after purification. On the other hand, an appreciable amount (up to 2.3%) of complex **1** was obtained in the pure form when acetonitrile or butyronitrile was used as the solvent (Table 1). However, all our attempts to improve the yield of **1** in these solvents have failed, suggesting sulfolane as the best solvent found so far for direct tricyanovinylation reaction of ferrocene. Interestingly, direct tricyanovinylation of ferrocene is extremely sensitive to the reaction time. Indeed, an increase of the reaction time to 20 min even at 100 °C leads to a dramatic decrease of the yield of compound **1**, which has never been isolated in appreciable quantities if the reaction is carried out for more than 30 min. A similar situation was observed when the reaction temperature was kept below 60 °C. In all our attempts, the direct tricyanovinylation reaction of ferrocene produced the orange

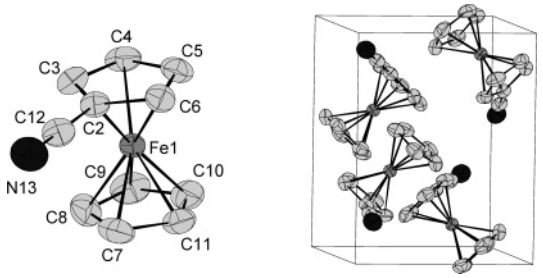

Figure 4. Molecular structure of complex **2**.

cyanoferrocene **2** as the major product with a typical yield of ca. 40% along with a small amount of unreacted ferrocene. Formation of arylcyanides in the tricyanovinylation reaction of aromatic compounds[17] and particularly in metallocenes (methods 1, 2, and 4, Scheme 1)[2−5,15,18] has never been reported in the literature and could be indicative of a different reaction mechanism in our case. Typically, the tricyanovinylation of aromatic compounds by TCNE requires the initial formation of an aryl−TCNE π-complex followed by nucleophilic attack of the olefin with the final elimination of HCN.[19] A similar reaction mechanism was postulated for the reaction between thallium cyclopentadienide and TCNE (Scheme 2).[4]

This reaction mechanism, however, cannot explain the formation of cyanoferrocene **2** as the major product in the reaction between FcH and TCNE, because it requires the thermodynamically unfavorable rearrangement of a highly conjugated stable tricyanovinylferrocenyl fragment. On the other hand, the high temperature required for the tricyanovinylation of ferrocene, formation of complex **2**, and the absence of a preferable tricyanovinylation site in the earlier reported[5] reaction between ethylferrocene and TCNE suggest the importance of a radical mechanism in the tricyanovinylation reaction of ferrocene. Such a radical reaction can follow, at least in theory, radical chain or single-electron-transfer mechanisms presented in Schemes 3 and 4.

Although the mechanism shown in Scheme 3 cannot be completely excluded, its importance for the tricyanovinylation reaction of ferrocene can be ruled out on the basis of the following considerations. According to Scheme 3, the only expected reaction product should be cyanoferrocene **2** because the formation of a tricyanovinyl radical requires an unfavorable elimination of a R−CN fragment. Moreover, since the formation of a cyanide radical can be accelerated in the presence of radical chain reaction initiators, the overall yield of complex **2** should be higher than that in a reaction without radical initiators. Addition of the radical initiators (i.e., benzoyl peroxide), however, did not significantly change the overall yield as well as the relative ratio of compounds **1** and **2** in the tricyanovinylation reaction of ferrocene. On the other hand, the single-electron-transfer mechanism presented in Scheme 4 can clearly explain the formation of complexes **1** and **2** in the reaction mixture. Moreover, this mechanism also explains an independence of the ratio of reaction products **1** and **2** from the external radical initiators. The first step involves the formation of the

(17) Robinson, M. J. T.; Rosenfeld, S. M. *Tetrahedron Lett.* **1975**, 1431. Raposo, M. M. M.; Sousa, A. M. R. C.; Kirsch, G.; Ferreira, F.; Belsley, M.; de Matos Gomes, E.; Fonseca, A. M. C. *Tetrahedron* **2005**, *61*, 11991. Lambert, C.; Gaschler, W.; Schmälzlin, E.; Meerholz, K.; Bräuchle, C. *J. Chem. Soc., Perkin Trans. 2* **1999**, 577.

(18) Hays, M. L.; Burkey, D. J.; Overby, J. S.; Hanusa, T. P.; Sellers, S. P.; Yee, G. T.; Young, V. G., Jr. *Organometallics* **1998**, *17*, 5521.

(19) Nogami, T.; Nakano, Y.; Hasegawa, Y.; Shirota, Y.; Mikawa, H. *Bull. Chem. Soc. Jpn.* **1979**, *52*, 2110. Rappoport, Z.; Rav-Acha, C. *Tetrahedron Lett.* **1984**, *25*, 117.

Table 3. Selected Bond Distances (Å) and Angles (deg) of Complex 1

	293 K	173 K
Fe1−C1	2.0296(15)	2.033(5)
Fe1−C2	2.0298(11)	2.024(3)
Fe1−C3	2.0548(11)	2.047(3)
Fe1−C4	2.0577(17)	2.057(4)
Fe1−C5	2.0529(11)	2.052(3)
Fe1−C6	2.0442(13)	2.039(3)
C1−C2	1.4349(16)	1.426(4)
C2−C3	1.4172(18)	1.399(5)
C3−C3′	1.407(3)	1.406(7)
C4−C5	1.4167(18)	1.413(4)
C5−C6	1.421(2)	1.419(5)
C6−C6′	1.422(3)	1.405(7)
C1−C7	1.473(2)	1.460(7)
C7−C8	1.358(3)	1.359(8)
C7−C9	1.453(5)	1.513(19)
C8−C10	1.425(5)	1.394(19)
C8−C11	1.491(3)	1.503(8)
N1−C9	1.154(11)	1.11(3)
N2−C10	1.095(11)	1.15(3)
N3−C11	1.094(3)	1.091(7)
C1−C2−C3	107.32(11)	107.9(3)
C2−C3−C3′	108.76(8)	108.5(2)
C2−C1−C2′	107.80(14)	107.2(4)
C4−C5−C6	108.37(12)	107.7(3)
C5−C6−C6′	107.75(8)	108.2(2)
C5−C4−C5′	107.74(17)	108.3(4)
C2−C1−C7	112.06(10)	112.7(3)
C1−C7−C8	123.48(18)	124.3(5)
C1−C7−C9	119.8(2)	119.2(7)
C7−C9−N1	178.2(7)	178.1(16)
C8−C10−N2	176.9(8)	175.8(15)
C8−C11−N3	157.75(11)	157.8(3)
C7−C8−C10	123.4(3)	122.3(8)
C7−C8−C11	115.1(2)	115.4(5)
C10−C8−C11	121.5(2)	122.3(8)
C1−C2−C5−C4	0.04	0.55
C2−C1−C7−C8	1.26	1.78
C1−C7−C8−C10	3.33	3.67

Table 4. Selected Bond Distances (Å) and Bond Angles (deg) for Complex 2

distance		angle	
Fe1−C2	2.018(2)	C2−C3−C4	107.4(2)
Fe1−C3	2.032(3)	C3−C4−C5	108.8(2)
Fe1−C4	2.055(3)	C4−C5−C6	108.6(3)
Fe1−C5	2.053(3)	C2−C6−C5	106.7(3)
Fe1−C6	2.034(3)	C3−C2−C6	108.5(2)
Fe1−C7	2.032(3)	C7−C8−C9	107.5(3)
Fe1−C8	2.032(3)	C8−C9−C10	108.0(3)
Fe1−C9	2.037(3)	C9−C10−C11	108.6(3)
Fe1−C10	2.039(3)	C7−C11−C10	107.6(3)
Fe1−C11	2.041(3)	C8−C7−C11	108.3(3)
C2−C3	1.424(3)	C3−C2−C12	125.4(2)
C3−C4	1.409(4)	C6−C2−C12	126.0(2)
C4−C5	1.414(4)	C2−C12−N13	179.4(3)
C5−C6	1.419(4)		
C2−C6	1.435(4)	C7−Fe1-C2−C12	−6.08
C7−C8	1.410(5)		
C8−C9	1.407(5)		
C9−C10	1.399(5)		
C10−C11	1.401(4)		
C7−C11	1.403(4)		
C2−C12	1.432(4)		
C12−N13	1.139(3)		

well-known FcH−TCNE π-complex.[20] The next single-electron-transfer step results in formation of a $[FcH]^+[TCNE]^{\bullet-}$ ion pair. This step can be confirmed by UV−vis spectroscopy because of the expected presence of a well-resolved vibrational progression of $[TCNE]^{\bullet-}$ centered at ca. 425 nm.[21] Indeed, the recorded UV−vis spectra of the reaction mixture in sulfolane or acetonitrile at 80 °C immediately after the mixing of the reactants (Figure 2) clearly indicated the formation of the vibronically well-structured band observed at 425 nm. This band position along with its structure and clear vibrational progression with ca. 530 cm^{-1} interval and 14 vibrational components out of 17 expected leaves no doubt about the formation of a $[FcH]^{\bullet+}$-$[TCNE]^{\bullet-}$ anion-radical pair at the initial step of the tricyanovinylation reaction. In the next step, homolytic cleavage of the C−CN bond in the $[TCNE]^{\bullet-}$ radical-anion leads to the formation of cyano and tricyanovinyl radicals, which by analogy with well-documented reactions of ferricinium and carbon-centered free radicals[22] results in the formation of compounds **1** and **2** as reaction products (Scheme 4).

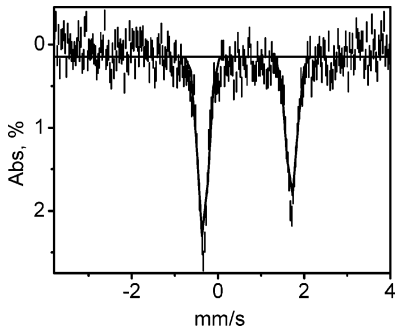

Figure 5. Room-temperature Mössbauer spectrum of complex **1**.

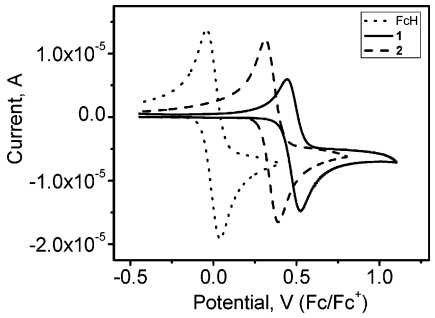

Figure 6. Cyclic voltammetry data on the Fe^{II}/Fe^{III} couple in ferrocene (dotted line, 0 V, Fc/Fc^+), complex **2** (dashed line, +0.349 V, Fc/Fc^+), and complex **1** (solid line, +0.484 V, Fc/Fc^+).

Overall, the optimization of the tricyanovinylation reaction of ferrocene by TCNE allows a one-step preparation of complex **1** in reasonable yield. Unlike previously discussed preparative procedures, the highly toxic mercury- or thallium-containing intermediates are now eliminated from the synthesis of **1**. The proposed reaction mechanism for the formation of complexes **1** and **2** requires a single-electron-transfer step followed by the formation of carbon-centered free radicals. Since only scarce characterization data are available in the literature for complex **1**, we decided to characterize this interesting compound in detail.

2. Spectroscopy, Redox Properties, Electronic, and Molecular Structures of Complexes 1 and 2. It has been reported[23] that (octamethylferrocenylmethylene)malononitrile, which is structurally close to compound **1**, undergoes phase transformation at ∼220 K, leading to a significant change in

(20) Frey, J. E.; Du Pont, L. E.; Puckett, J. J. *J. Org. Chem.* **1994**, *59*, 5386.

(21) Del Sesto, R. E.; Miller, J. S.; Lafuente, P.; Novoa, J. J. *Chem. Eur. J.* **2002**, *8*, 4894.

(22) Baciocchi, E.; Floris, B.; Muraglia, E. *J. Org. Chem.* **1993**, *58*, 2013. Lampard, C.; Murphy, J. A. *Tetrahedron Lett.* **1991**, *32*, 4993. Little, W. F.; Lynn, K. N.; Williams, R. *J. Am. Chem. Soc.* **1963**, *85*, 3055. Bin Din, L.; Meth-Cohn, O.; Walshe, N. D. *Tetrahedron Lett.* **1979**, 4783.

(23) Laus, G.; Schottenberger, H.; Wurst, K.; Herber, R. H.; Griesser, U. *J. Phys. Chem. B* **2004**, *108*, 5082.

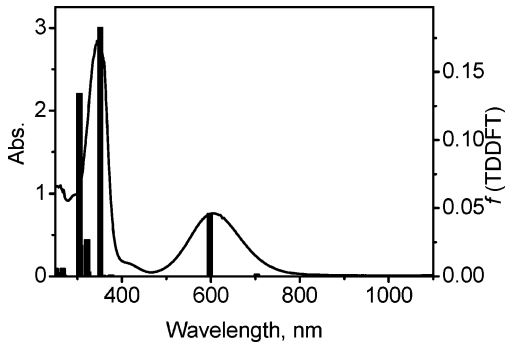

Figure 7. UV−vis spectrum (solid line) and TDDFT-predicted vertical excitation energies (vertical bars) of complex **1** in acetone.

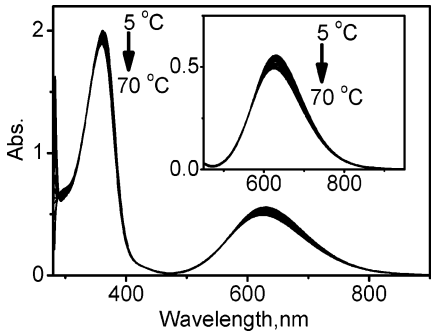

Figure 8. Variable-temperature UV−vis spectra of complex **1**.

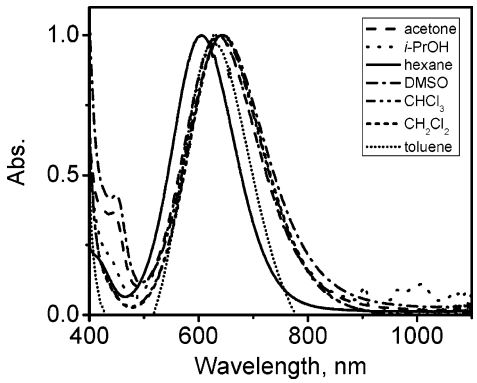

Figure 9. Normalized absorption of complex **1** (400−1100 nm) in selected solvents.

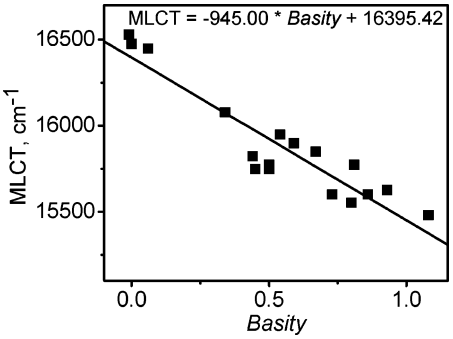

Figure 10. Correlation between experimental low-energy band position in complex **1** and Swan's solvent *Basity* parameter (r = 0.927, sd = 125.85 cm^{-1}).

its molecular structure, clearly observed by X-ray crystallography. Thus, in order to find out whether or not compound **1** has a similar phase transition, we conducted X-ray crystallography experiments on this complex at 293 and 173 K. The CAMERON diagram of compound **1** is presented in Figure 3,

Table 5. UV−vis Maxima for the Lowest Energy Band in Complex 1 in Different Solvents along with Solvent Parameters and Transition Energies

solvent[a]	λ_{max} (cm^{-1})	E_T (kJ/mol)	α	β	π^*
hexane	16 529	197.7	0	0	−0.04
heptane	16 474	197.1	0	0	−0.08
cyclohexane	16 447	196.8	0	0	0
diethylether	16 077	192.3	0	0.47	0.27
toluene	15 948	190.8	0	0.11	0.54
ethylacetate	15 898	190.2	0	0.45	0.55
THF	15 848	189.6	0	0.55	0.58
2-propanol	15 823	189.9	0.76	0.84	0.48
1,2-dimethoxyethane	15 773	188.7	0	0.41	0.53
acetone	15 773	188.7	0.08	0.43	0.71
methanol	15 748	188.4	0.98	0.66	0.6
ethanol	15 748	188.4	0.86	0.75	0.54
butyronitrile	15 699	187.8	0	0.4	0.71
DMF	15 625	186.9	0	0.69	0.88
acetonitrile	15 600	186.6	0.19	0.4	0.75
chloroform	15 600	186.6	0.2	0.1	0.58
dichloromethane	15 552	186.0	0.13	0.1	0.82
o-dichlorobenzene	15 552	186.0	0	0.03	0.8
DMSO	15 480	185.8	0	0.76	1
1,1,2,2-tetrachloroethane	15 244	182.4	0	0	0.95

[a] Solvent parameters are taken from ref 28.

while selected metric parameters are listed in Table 3. The crystal structures of cyanovinyl ferrocenes are extremely rare in the literature.[24] Indeed, complex **1** represents the only known example of a vinylferrocene with a cyano group connected to the α-carbon atom of the vinyl fragment. At both temperatures, compound **1** crystallizes in the same centrosymmetric monoclinic $P2_1/m$ unit cell with virtually the same parameters, adopting two molecules in the unit cell with one being unique (Table 2).

The iron atom along with ferrocene C(1) and C(4) atoms and one cyano group have been localized at special positions, while the rest of the tricyanovinyl group has been positionally disordered between two sites, which are symmetry related through a mirror plane. The observed iron−carbon distances are in an expected range and well comparable to numerous ferrocene derivatives. Interestingly, the Fe(1)−C(1) and Fe(1)−C(2) distances are slightly shorter than other Fe(1)−C(*n*) distances in the ferrocene fragment probably because of the presence of the strong electron-withdrawing tricyanovinyl group. The observed ferrocene conformation is clearly eclipsed at both temperatures tested, and the tricyanovinyl substituent is almost coplanar with the neighboring cyclopentadiene ring. The last observation is in contrast to the structure of (octamethylferrocenylmethylene)malononitrile, in which the torsion angle between the ferrocene core and dicyanovinyl substituent varies between 37° and 41°.[23]

Unlike many other ferrocene-containing structures,[24] there is no disorder observed in the ferrocene fragment. The vinyl carbon−carbon bond is clearly double bond in nature, with an observed distance of ∼1.36 Å. The carbon−nitrogen bonds and C−C−N angles in the tricyanovinyl fragment have been observed in expected ranges for triple bonds and angles, respectively. Finally, numerous intermolecular contacts were found between tricyanovinylferrocene substituents in neighboring molecules, but accurate identification of those was affected by the positional disorder of this substituent in the solid state.

The room-temperature X-ray structure of compound **2** is presented in Figure 4, while the most important distances and

(24) CCDC data base V5.27, November 2006, Cambridge, UK.

Table 6. Correlations Between Observed MLCT Band Energy in Complex 1 and Kamlet−Taft Model Parameters

parameter	eq 2	eq 3	eq 4
a	−207.92	−198.33	−110.78
b	212.92	178.78	
s	−1118.72	−1098.04	−1041.83
d	40.60		
r^2	0.948	0.948	0.933
sd	86.29	83.97	92.17

angles are listed in Table 4. The ferrocene fragment was found in the eclipsed conformation with a torsion angle of 6.08°. All iron−carbon bonds were observed in a narrow region (2.018−2.055 Å), with the Fe(1)−C(2) bond being significantly shorter than all others in the ferrocene core. The cyano group has usual geometry with a C(2)−C(12)−N(13) angle of 179.4° and C(2)−C(12) and C(12)−N(13) bond distances of 1.432 and 1.139 Å, respectively.

NMR, IR, and Mössbauer Spectra of Compounds 1 and 2. The ^{1}H NMR spectrum of complex **1** in $CDCl_3$ consists of three signals centered at 5.27, 5.16, and 4.48 ppm, while nine signals were observed in the ^{13}C NMR spectrum (Figures SI1 SI2). All three cyano group carbons are clearly resolved and observed in a narrow region between 113.22 and 113.74 ppm, along with signals at 143.98 and 79.78 ppm observed for carbons of the vinyl group. The ultimate assignment of the ferrocenyl fragment has been done on the basis of the gHMQC spectrum (Figure SI3). Indeed, the protons in the unsubstituted cyclopentadienyl ring located in the ^{1}H spectrum at 4.48 ppm clearly correlate with the signal at 73.19 ppm in the ^{13}C NMR spectrum. The ^{1}H signal at 5.27 ppm correlates with the peak observed at 77.79 ppm in the ^{13}C NMR, while the ^{1}H signal at 5.16 ppm correlates with the peak located at 72.15 ppm in the ^{13}C NMR. Finally, the ipso-carbon can be assigned to the signal at 75.24 ppm in the ^{13}C NMR (Figure SI2). The ^{1}H NMR spectrum of compound **2** consists of two signals observed at 4.65 and 4.39 ppm, corresponding to the substituted cyclopentadienyl ring and a signal observed at 4.34 ppm corresponding to the protons of the unsubstituted ring (Figure SI4). The peak of the carbon atom of the cyano group was found at 120.20 pm in the ^{13}C NMR spectrum, while the other peaks were assigned on the basis of the gHMQC correlation. Indeed, gHMQC correlates protons in the unsubstituted cyclopentadienyl ring with a peak at 70.54 ppm observed in the ^{13}C NMR spectrum and ^{1}H signals at 4.65 and 4.39 ppm with ^{13}C peaks at 71.68 and 70.69, respectively (Figure SI6). The presence of Cp-H protons (band at 3100 cm^{-1}, ν_{Cp-H}), cyano groups (strong band at 2222 cm^{-1}, ν_{CN}), and a conjugated C═C bond (strong band at 1526 cm^{-1}, $\nu_{C=C}$) in **1** was also confirmed by IR spectroscopy. Similarly, the observed frequencies in **2** for Cp-H and cyano group vibrations (3092 and 2224 cm^{-1}, respectively) are close to those observed in the case of **1**. Similar to many other ferrocene derivatives,[25] the Mössbauer spectrum of **1** consists of an asymmetric doublet with an isomer shift of 0.42 mm/s (relative to α-Fe) and a quadrupole splitting of 2.05 mm/s (Figure 5). Interestingly, the asymmetry of the Mössbauer doublet in compounds **1** and **2** are different: in the case of **1** the low-energy component of the doublet is more intense, but the opposite is observed in the case of **2**. This difference will be explained below on the basis of DFT calculations.

Finally, complexes **1** and **2** undergo one-electron Fe^{II}/Fe^{III} oxidation in electrochemical conditions, as can be seen from cyclic voltammetry experiments presented in Figure 6. The electron-withdrawing nature of cyano- and tricyanovinyl groups results in higher oxidation potentials for **1** and **2** as compared to the parent ferrocene. Indeed, to the best of our knowledge, complex **1** has the highest Fe^{II}/Fe^{III} oxidation potential for monosubstituted ferrocene derivatives.[26]

Overall, shifts of Cp-H protons to low-field in the NMR spectrum of **1** as compared to **2**, the higher Fe^{II}/Fe^{III} oxidation potential of **1**, and its lower quadrupole splitting (following Silver's hypothesis on the relationship between quadrupole splitting in the oxidation potentials in ferrocenes[26]) in the Mössbauer spectrum (2.05 mm/s compared to 2.36 mm/s observed in **2**) point out a stronger electron-withdrawing power of the tricyanovinyl group as compared to the cyano substituent.

UV−vis Spectra and Solvatochromism of Compound 1. The electronic spectra of compound **1** in a variety of solvents consists of two intense bands in the UV−vis region (Figure 7). The first low-energy band was tentatively assigned to a metal-to-ligand charge-transfer (MLCT) transition, while the most intense band observed at ca. 360 nm to a $\pi-\pi^*$ transition.[2] The MLCT band is slightly thermochromic, with a 5 nm shift and 12% loss in intensity observed in toluene for a 5 to 70 °C range, Figure 8. One of the most interesting features of complex **1** is that the low-energy optical transition exhibits significant positive solvatochromic behavior (i.e., increase in the solvent

Table 7. Atomic Orbital Contributions into MOs in Complexes 1, 2, and Ferrocene[a]

MO	symmetry	*E*, eV	Fe, %	Cp, %	substituent
		Complex **1**			
66	A	−8.218	11.4	38.9	49.7
67	A	−7.739	34.7	65.1	0.3
68	A	−7.507	25.8	55.6	18.6
69	A	−7.060	7.4	92.1	0.4
70	A	−6.817	7.1	56.2	36.8
71	A	−5.503	79.9	14.0	6.1
72	A	−5.343	67.0	30.3	2.7
73	***A***	***−5.306***	***67.1***	***32.6***	***0.4***
74	A	−3.824	11.3	11.5	77.2
75	A	−2.274	40.7	53.9	5.4
76	A	−2.256	40.9	53.9	5.2
77	A	−1.916	1.5	10.3	88.2
		Complex **2**			
48	A	−7.202	32.1	66.9	1.0
49	A	−7.109	31.2	61.3	7.5
50	A	−6.634	7.0	93.0	0.0
51	A	−6.436	6.0	77.5	16.5
52	A	−4.946	87.8	11.0	1.2
53	A	−4.794	59.5	39.1	1.4
54	***A***	***−4.725***	***64.5***	***35.3***	***0.2***
55	A	−1.913	43.9	50.8	5.2
56	A	−1.767	42.9	56.7	0.4
57	A	−0.626	10.0	73.7	16.3
58	A	0.167	0.7	59.7	39.6
59	A	0.435	2.2	97.4	0.4
		Ferrocene (D_{5h})			
39, 40	E_2'	−9.001	0.0	100.0	
41	A_2''	−8.585	10.6	89.4	
42, 43	E_1''	−6.489	31.6	68.4	
44, 45	E_1'	−6.013	6.2	93.8	
46	A_1'	−4.371	86.9	13.1	
47, 48	***E_2'***	***−4.168***	***61.6***	***38.4***	
49, 50	E_1''	−1.318	42.6	57.4	
51, 52	E_2''	0.831	0.0	100	
53	A_1'	0.848	46.9	53.1	
54, 55	E_2'	0.954	8.7	91.3	

[a] The HOMO is labeled in bold, italics.

(25) Fluck, E. In *Chemical Applications of Mössbauer Spectroscopy*; Goldanskii, V. I., Herber, R. H., Eds.; Academic Press, Inc.: New York, 1968; pp 268−311.

(26) Robarts, R. M. G.; Silver, J. *J. Organomet. Chem.* **1984**, *263*, 235.

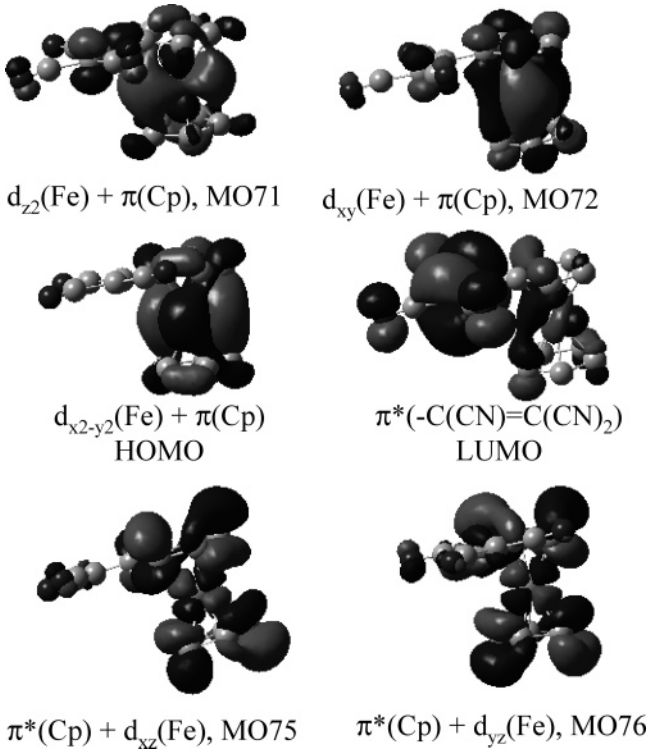

Figure 11. Frontier molecular orbitals of complex **1**.

polarity leads to the lower transition energy), with a maximum observed solvatochromic shift of 1285 cm^{-1} (Figure 9). The solvatochromic effect observed for compound **1** is about twice as large as compared to that found in the (octamethylferrocenylmethylene)malononitrile[23] and is comparable to the solvatochromic shift in the 2-nitro-3-(octamethylferrocenyl)-acrylonitrile.[27]

In the solid state, compound **1** is deep blue, and the solution color changes depending on the solvent. Complex **1** is navy blue in hexane and cyclohexane, while it is deep blue in dichloromethane and chloroform. The high-energy band located at ca. 360 nm, on the other hand, shows little solvatochromism, confirming its predominantly $\pi-\pi^*$ nature.

The electronic absorption spectra of compound **1** in 20 solvents of different polarity are summarized in Table 5. In order to compare the solvatochromic properties of compound **1** with those known for other ferrocene-containing complexes of general formula Fc−C(R)═CXY, where X and Y are electron-withdrawing groups, we also presented molar transition energies, E_T (as calculated using eq 1), in the same table.

$$E_T\ (\text{kJ mol}^{-1}) = hcN/\lambda = 119\,625/\lambda\ (\text{nm}) \qquad (1)$$

We attempted to correlate the experimentally observed energy of the low-energy band in compound **1** with various empirical solvent parameters as well as experimentally derived constants. The solvent scales such as Kosower's Z,[28] Reichard's $E_T(30)$ MLCT,[29] Gutmann's AN and DN,[30] dipole moment of solvents,[31] Swain's *Acity* parameter,[32] and Eisenberg's empirical Pt(NN)(SS)[33] gave considerably poor correlations with experimental data for **1** (Figure SI8). On the other hand, the energy of the color-defining band near 630 nm linearly correlates with Swain's *Basity* scale[33] (Figure 10).

The band position can also be related with the Kamlet−Taft model (eqs 2−4):[34]

$$E\ (\text{cm}^{-1}) = E^\circ + s(\pi^* + d\delta) + a\alpha + b\beta \qquad (2)$$

$$E\ (\text{cm}^{-1}) = E^\circ + s\pi^* + a\alpha + b\beta \qquad (3)$$

$$E\ (\text{cm}^{-1}) = E^\circ + s\pi^* + a\alpha \qquad (4)$$

where E°, s, d, a, and b are the coefficients determined from regression analysis, α is the hydrogen-bond donation ability of the solvent, β is the hydrogen-bond acceptance ability of the solvent; π^* is a parameter that describes the polarity and polarizability of the solvent, and the δ term is dependent on the class of solvent to be studied as defined by Taft. Often, the contribution from the last term is negligibly small, which leads to the modified Kamlet−Taft expression shown in eq 3.[23] These two equations when correlated with the experimental data led to a correlation coefficient of $r^2 = 0.948$ for both eqs 2 and 3 (Table 6). It has also been suggested[23] that in the case of the substituted vinylferrocenes the hydrogen-bond acceptance parameter β is negligibly small and can be ignored in the regression analysis, which describes solvatochromic properties of these compounds. Indeed, the correlation coefficient of $r^2 = 0.933$ has been observed only if the parameters π^* and α were taken into consideration. Further analysis of the correlation equation, however, clearly indicates that the influence of the hydrogen-bond donation parameter α is also small as compared to the parameter π^*, and the correlation coefficient of $r^2 = 0.927$ was observed only if the parameter π^* has been considered. Thus, the polarity and polarizability are the major factors, which can explain the solvatochromic properties of compound **1**.

Electronic Structures of Complexes 1 and 2 as Compared to Ferrocene. In order to gain insight into the electron-withdrawing strength of the tricyanovinyl group and explain the observed spectroscopic properties of complex **1**, we have calculated the electronic structures of **1** and **2** at the DFT level and compared those to the well-known electronic structure of ferrocene calculated at the same level of theory.

The compositions of selected molecular orbitals of **1**, **2**, and ferrocene are listed in Table 7, while frontier molecular orbitals of **1** are depicted in Figure 11. As expected for the low-spin iron(II) derivatives of ferrocene,[35] the HOMO and HOMO−1 belong to the iron-centered $d_{x^2-y^2}$ and d_{xy} orbitals followed by the d_{z^2} orbital (HOMO−2). The introduction of the electron-withdrawing cyano and trivinylcyano groups into the ferrocene ring stabilizes these occupied metal-centered orbitals. For instance, the HOMO energy in **1** is ∼1.1 eV lower than that in the parent ferrocene and ∼0.6 eV lower than that in **2**, in excellent agreement with NMR, Mössbauer, and electrochemical data provided above, suggesting that the electron-withdrawing strength increases in the order −H < −CN < −C(CN)═C(CN)$_2$. Next, the degeneracy of $d_{x^2-y^2}$ and d_{xy} orbitals in the parent ferrocene disappears in **1** and **2**, although the calculated splitting of these orbitals is only 0.07 and 0.04 eV, respectively. In all cases, the metal-centered occupied orbitals are well-separated from the first pair of occupied cyclopentadienyl-centered π-orbitals, which is degenerated in the case of ferrocene

(27) Laus, G.; Schottenberger, H.; Schuler, N.; Wurst, K.; Herber, R. H. *J. Chem. Soc., Perkin Trans. 2* **2002**, 1445.
(28) Marcus, Y. *Chem. Soc. Rev.* **1993**, *22*, 409.
(29) Kosover, E. *J. Am. Chem. Soc.* **1958**, *80*, 3253.
(30) Reichardt, C. *Angew. Chem., Int. Ed. Engl.* **1965**, *4*, 29.
(31) Mayer, U.; Gutmann, V.; Gerger, W. *Monatsh. Chem.* **1975**, *106*, 1235. Gutmann V.; Wychera, E. *Inorg. Nucl. Chem. Lett.* **1966**, *2*, 257.
(32) *The Merck Index*, 14th ed.; Merck Publishing Inc., 2006.
(33) Swain, C. G.; Swain, M. S. *J. Am. Chem. Soc.* **1983**, *105*, 502.
(34) Cummings, S. D.; Eisenberg, R. *J. Am. Chem. Soc.* **1996**, *118*, 1949.
(35) Kamlet, M. J.; Abboud, J.-L. M.; Taft, R. W. *J. Am. Chem. Soc.* **1977**, *99*, 6027.

Table 8. Vertical Excitation Energies of Complex 1 Calculated Using the TDDFT Approach[a]

transition	λ, nm	f	transitions and expansion coefficients[b]
1	811.30	0.0001	**73** → **74**, 0.69192
2	749.24	0.0015	71 → **74**, 0.35239; 72 → **74**, 0.58308
3	616.97	0.0465	70 → **74**, 0.16512; 71 → **74**, 0.54737; 72 → **74**, −0.29074
4	400.37	0.0003	72 → 75, −0.43223 ; **73** → 76, 0.54888
5	400.18	0.0000	72 → 75, 0.55556; **73** → 76, 0.43298
6	387.58	0.0000	71 → 75, 0.50225; 72 → 75, −0.30031; **73** → 76, 0.36653
7	378.52	0.0005	70 → **74**, 0.10284; 71 → 76, −0.14392; 72 → 76, −0.15579 ; **73** → **74**, 0.65865
8	375.55	0.0011	70 → **74**, −0.12133; 71 → 75, 0.10425; 71 → 76, 0.64474; **73** → **74**, 0.19434
9	366.59	0.0036	70 → **74**, −0.11547; **73** → **74**, 0.67760
10	361.53	0.0003	72 → **74**, 0.70158
11	358.19	0.1504	68 → **74**, 0.34362; 70 → **74**, −0.12514; 69 → **74**, 0.51523; **73** → **74**, 0.15367
12	345.69	0.0052	71 → 76−0.11470; 71 → **74**, 0.67559
13	325.13	0.0146	68 → **74**, −0.27262; 67 → **74**, 0.13622; 71 → 75, 0.13045; 71 → 76−0.19899; 71 → **74**, −0.12597; 72 → 75, −0.32369; **73** → 76, 0.35199;
14	323.32	0.0119	67 → **74**, −0.31042; 71 → 75, 0.21983; 71 → 76, −0.19930; 71 → **74**, −0.10293; 72 → 75, 0.21420; 72 → 76, 0.27546; **73** → 75, 0.27109; **73** → 76, −0.12307
15	308.12	0.1007	69 → **74**, 0.19519; 67 → **74**, 0.23279; 68 → **74**, −0.47144; 70 → **74**, 0.20252; 71 → 76, −0.14279; 72 → 75, −0.11606; **73** → 76, 0.156**74**
16	306.25	0.0446	67 → **74**, 0.51165; 68 → **74**, 0.24126; 69 → **74**, −0.11634; 71 → 75, 0.16128; 71 → 76, −0.13689; 72 → 76, 0.13101; **73** → 75 0.15521

[a] Only energies above 300 nm are shown. [b]HOMO and LUMO are labeled in bold.

Table 9. Experimental and DFT-Predicted Mössbauer Isomer Shifts and Quadrupole Splittings in Complexes 1, 2, and Ferrocene

	electric field gradient tensor elements (au)			quadrupole splittings ΔE_Q (mm s^{-1})			isomer shift δ (mm s^{-1})		anisotropic parameter η (mm s^{-1})	
	V_{11}	V_{22}	V_{33}	calc	exptl	ρ_{Fe} (au)	calc	exptl	calc	exptl
1	−1.292	0.389	0.903	2.15	2.05	11615.9800	0.55	0.42	0.398	
2	−1.408	0.651	0.757	2.28	2.36	11615.9713	0.55	0.52	0.075	
FcH	−1.442	0.721	0.721	2.34	2.40	11615.8703	0.60	0.53	0.000	0

and nearly degenerated in the case of compounds **1** and **2**. These π-orbitals play an important role in the observed UV−vis spectrum of compound **1** as discussed below, while their contribution to the stability of the ferrocenyl-containing system is expected to be small.[9,36] The next pair of occupied orbitals has appreciable overlap with the metal d orbitals and, thus, can act as a significant π-donor in the bonding scheme of complexes **1** and **2**. In the case of the parent ferrocene and **2**, the LUMO and LUMO+1 are predominantly metal centered d_{xz} and d_{yz} orbitals, respectively, with significant contribution from the cyclopentadienyl ligands, thus suggesting that the lowest energy transitions in these compounds should be d−d in nature, in agreement with the experimental data.[36] In the case of tricyanovinylferrocene, however, the LUMO consists of the π-orbital localized on the tricyanovinyl fragment, while the predominantly metal-centered d_{xz} and d_{yz} orbitals form LUMO+1 and LUMO+2 (Figure 11). The presence of the ligand-based low-energy π-orbital is responsible for the possible low-energy metal-to-ligand charge-transfer bands observed in the UV−vis spectrum of compound **1**, which is discussed below on the basis of TDDFT calculations.

The TDDFT-predicted electronic absorption spectrum of complex **1** is presented in Table 8 and graphically in Figure 7. The presence of three closely spaced predominantly metal-centered HOMO to HOMO−2 orbitals and the low-lying tricyanovinyl-localized LUMO resulted in three low-energy transitions with theoretical vertical excitation energies close to the low-energy band observed in the UV−vis spectrum of **1**. Out of these three transitions, the first two, which predominantly consist of d_{xy} or $d_{x^2-y^2}$ to LUMO excitations, have small oscillator strengths, apparently because of the negligible overlap between these orbitals. The third transition, which predominantly consists of d_{z^2} to LUMO excitation, has a relatively high oscillator strength and perfectly agrees with the position of the low-energy band observed in the UV−vis spectrum of **1**. A similar trend in MLCT band intensities has recently been observed in the case of molybdenum(0) complexes.[37] The most intense band predicted by the TDDFT approach for the UV−vis spectrum of **1** predominantly consists of $\pi-\pi^*$ transitions from occupied π orbitals of the ferrocene ligand to the LUMO and correspond to the UV band observed at ca. 360 nm in the UV−vis spectrum of **1** (Table 8). Predominant $\pi-\pi^*$ character of these transitions is in excellent agreement with the small solvatochromism of the experimentally observed ∼360 nm band in **1**. Overall, TDDFT-predicted vertical excitation energies and the experimentally observed UV−vis spectrum of **1** are in excellent agreement with each other (Figure 7).

The calculated Mössbauer parameters and electric field

(36) Martin, C. H.; Zerner, M. C. In *Inorganic Electronic Structure and Spectroscopy*; Lever, A. B. P., Solomon, E. I., Eds.; John Wiley and Sons: New York, 1999; Vol. I, p 555.

(37) Armstrong, A. T.; Smith, F.; Elder, E.; McGlynn, S. P. *J. Chem. Phys.* **1967**, *46*, 4321. Sohn, Y. S.; Hendrickson, D. C.; Gray, H. B. *J. Am. Chem. Soc.* **1971**, *93*, 3603. Grandberg, K. I.; Gubin, S. P.; Perevalova, E. G. *Izv. Acad. Nauk SSSR, Ser. Khim.* **1966**, 549.

(38) Nemykin, V. N.; Olsen, J. G.; Perepa, E.; Basu, P. *Inorg. Chem.* **2006**, *45*, 3557.

gradient tensor elements of **1**, **2**, and ferrocene are listed in Table 9. These values show an excellent agreement between theoretical and experimental data. An observed decrease in quadrupole splitting going from parent ferrocene to **2** and **1** is reproduced well by DFT calculations. More importantly, the large anisotropy of the Mössbauer doublet experimentally observed in **1** is also obvious in DFT results. Indeed, the presence of a large-size strong electron-withdrawing tricyanovinyl substituent in complex **1** leads to nonequivalence of V_{22} and V_{33} tensor elements and results in large anisotropy of the Mössbauer doublet. On the other hand, V_{22} and V_{33} tensor elements are equivalent or almost equivalent in the case of ferrocene and complex **2**, respectively, in excellent agreement with the experimental data.[25]

Conclusions

In this paper we have investigated the reaction between ferrocene and tetracyanoethylene as a function of solvent, temperature, and time in order to improve the yield of tricyanovinylferrocene **1**, which is used as a starting material for the preparation of unique ferrocenyl-containing tetraazaporphyrin complexes. Under optimized reaction conditions, the target compound can be prepared in ~26% yield by the reaction of 1 equiv of ferrocene and 2 equiv of tetracyanoethylene for 10 min in sulfolane at 110 °C along with the cyanoferrocene **2** as a major reaction product. It was suggested that the reaction follows a single-electron-transfer radical mechanism. The limited stability of the tricyanovinylferrocene in polar solvents was investigated by UV−vis spectroscopy. The possible phase transition in tricyanovinylferrocene has been tested by X-ray crystallography at 173 and 293 K, but it was found that in both cases tricyanovinylferrocene crystallizes in the monoclinic $P2_1/m$ group with similar unit cell parameters, while cyanoferrocene crystallizes in the orthorhombic $P2_12_12_1$ group. The prominent low-energy band observed in the UV−vis spectrum of tricyanovinylferrocene was unambiguously assigned to a metal-to-ligand charge-transfer transition on the basis of both experimental and theoretical (TDDFT) data, while its solvatochromic behavior was tested using the Kamlet−Taft model. It was found that the observed solvatochromism predominantly depends on the value of dipolarity/polarizability parameter π^* in the Kamlet−Taft equation. The superiority of electron-withdrawing strength of the tricyanovinyl group over the cyano substituent was confirmed using NMR, Mössbauer, and electrochemical experiments.

Acknowledgment. Generous support from the Research Corporation (Cottrell College Science Award CC6766), University of Minnesota Grant-in-Aid (Grant 20209), and Minnesota Supercomputing Institute to V.N.N. is greatly appreciated. We also wish to acknowledge Prof. Eric Oldfield and Prof. Viktor Zhdankin for the stimulation discussion, Dr. Victor Young for assistance with low-temperature X-ray data collection, and Dr. Ernst Polshin for assistance with Mössbauer experiments.

Supporting Information Available: Crystallographic data in CIF format, NMR spectra of complexes **1** and **2**, and single-parameter correlations between the energy of the MLCT band in complex **1** and different solvent parameters. This material is available free of charge via the Internet at http://pubs.acs.org.

OM070160K